Analysis of dynamic metasurface antennas under matching network constraints

Joseph Carlson*, Nitish V. Deshpande*, Miguel R. Castellanos[†], and Robert W. Heath Jr.*
*ECE Department, University of California San Diego (e-mail: {j4carlson, nideshpande, rwheathjr}@ucsd.edu)

†EECS Department, University of Tennessee, Knoxville (e-mail: mrcastellanos@utk.edu)

Abstract—Dynamic metasurface antennas (DMAs) are a type of waveguide-fed reconfigurable slot antenna with integrated tunable components that enable low-power beamforming. Despite recent advances made to optimize signal processing and beamforming with DMAs, there is minimal work investigating the improvement of the DMA matching efficiency. In this paper, we explore impedance matching for DMAs and extend previous impedance models for static slot antennas to the reconfigurable DMA. We also provide an optimization algorithm to increase the DMA matching efficiency without any external matching network or additional components. The simulation results show that the matching optimization procedure significantly improves the matching efficiency of DMAs with high coupling.

I. Introduction

DMAs radiate power through reconfigurable slot elements that can be tuned by an external controller [1]. Two common low-power reconfigurable components used for DMA elements are varactors and PIN diodes [2]. Tuning the reconfigurable component alters the resonant response of a DMA element, which can be leveraged to enable beamforming. Since the power consumption of the reconfigurable components is minimal compared to typical beamforming hardware, such as phase shifters, DMAs can be scaled up to create large, highly energy-efficient antenna arrays [3].

Travelling-wave slot antennas are typically matched based on the isolated impedance or admittance of the individual slot elements [4]. The most common waveguide-fed slot element, the longitudinal slot, is modeled as an isolated shunt admittance on a waveguide [5], [6]. The total admittance can then be calculated by adding up the admittances of all individual slot elements [7]. Prior methods to determine the total input admittance of the slot antenna array, however, assumes static slot elements that cannot be reconfigured. We incorporate reconfigurable impedances and admittances into the DMA impedance model and provide a novel impedance matching technique that differs from conventional matching networks.

While static antennas often only require a fixed matching network to provide a sufficient impedance match, reconfigurable matching networks have been explored to provide higher matching efficiency and increase the functionalities of reconfigurable antennas [8]. Frequency-reconfigurable antennas with tunable matching networks in [9], [10] incorporate PIN diodes and varactors to increase the matching efficiency. Analytical formulas have also been derived for the coverage of different reconfigurable matching networks [11]. The tunable

matching networks designed in these works assume a reconfigurable antenna element with an isolated feed, such as a loop antenna. Reconfigurable slot elements differ from these antenna elements since there is a singular feed for all elements in the antenna array, and the source impedance for a slot antenna array is the characteristic waveguide impedance, rather than a source impedance from a coaxial cable feed. New techniques need to be developed to optimize the impedance matching for a reconfigurable slot antenna compared to independently-fed reconfigurable antenna elements.

In this paper, we develop a DMA impedance model and improve the matching efficiency of the DMA. We extend prior impedance models on static slotted-waveguide antennas to accurately calculate the effective impedance of the DMA array. This avoids the need for repetitive electromagnetic simulations to determine the DMA impedance. We then propose a novel method to optimize the matching efficiency of a DMA by configuring the DMA element weights to improve the impedance matching between the DMA array and the waveguide characteristic impedance. We show in simulation results that for DMA elements with large coupling, the proposed matching efficiency optimization algorithm increases the matching efficiency of the DMA.

Notation: For a complex number z, |z| is its magnitude, and $\angle z$ is its phase. The superscript ^a denotes an isolated element parameter. The term j denotes the imaginary unit.

II. DMA IMPEDANCE AND BEAMFORMING MODEL

We describe the impedance model for an isolated DMA slot element and the effective impedance of the entire DMA. The total effective impedance of a slotted-waveguide array is calculated based on the impedance of each isolated element. We extend the static slot antenna element impedance model to the reconfigurable case and determine the effects of the reconfigurability on the total effective DMA impedance. While the DMA has a frequency-selective response, we focus on DMA beamforming and impedance matching at a particular operating frequency $f_{\rm t}$ and omit the frequency-dependence of the DMA impedance and beamforming weights in notation.

A. DMA impedance model

Due to the large transverse width of the DMA element, the isolated impedance of a DMA element can be modeled as a transverse slot antenna element [4]. While analytical models exist to calculate the isolated impedance for a simple longitudinal or transverse slot antenna element [4], it is difficult to extend these models to DMAs because of the complexity of the DMA element geometry. Instead, we take a computational approach and calculate the isolated DMA element impedance based solely on its scattering parameters. Let $f_{\rm t}$ be the operating frequency for the DMA, $f_{\rm r,n}$ be the resonant frequency tuning for the nth DMA element, and $S_{11}^{\rm a}$ be the isolated reflection coefficient for the DMA element. We omit the dependence of the isolated impedance on $f_{\rm t}$ for brevity. The isolated impedance for the nth DMA element is [4]

$$Z_n^{\mathsf{a}} = \frac{2S_{11}^{\mathsf{a}}(f_{\mathsf{t}}, f_{\mathsf{r},n})}{1 - S_{11}^{\mathsf{a}}(f_{\mathsf{t}}, f_{\mathsf{r},n})}.$$
 (1)

The model in (1) provides a simple and accurate method to calculate the isolated DMA element impedance for any reconfigurable resonant frequency $f_{r,n}$. The reflection coefficient for a DMA element can be readily obtained either from full-wave electromagnetic simulations, or DMA models as described in [12].

The isolated impedance expression in (1) is valid for transverse slot elements and rotated slot elements with low scattering within the waveguide. To model a slot element as a series impedance, the scattering relationship $S_{12}^{\mathsf{a}} = 1 - S_{11}^{\mathsf{a}}$ must be satisfied [4], which provides a simple method to check the validity of the DMA element series impedance model. Empirically, we have found this to be true for DMA elements with low scattering through full-wave simulation results. The series impedance model, however, is an approximation of the more general Tee network model under low scattering conditions. Therefore, for DMA elements with high scattering, it is more accurate to model the DMA elements as a Tee network.

The appropriate impedance values for a Tee network can be obtained from the scattering parameters, and the total input impedance is calculated based on cascaded ABCD matrices for the DMA elements and waveguide [13]. We describe the impedance model as follows by assuming that scattering is low for the DMA elements to derive a simple, analytical expression for the total DMA impedance using the series impedance model. We note here that the same analysis can be done for high scattering elements with Tee networks and ABCD matrices, but the final impedance expression will be much more complex. We show results for both the Tee network and series impedance models in Section IV, as well as additional discussion on the validity of the models.

The waveguide can be modeled as a transmission line that carries the input signal from one DMA element to the next. The electrical length Θ of the effective transmission line between DMA elements is given by the waveguide propagation constant β_g and element spacing d as $\Theta = \beta_g d$ [13]. The total input impedance of the DMA can then be calculated recursively based on the reconfigurable isolated impedances of the DMA elements and the segments of waveguide transmission line. Fig. 1 shows the equivalent full circuit model for the

DMA [4]. Since we assume a waveguide-fed architecture, the characteristic impedance of the waveguide Z_0 is the effective source impedance for matching and is determined by the waveguide design. At the nth element, the effective DMA array impedance normalized by the characteristic waveguide impedance is [4]

$$\frac{Z_n}{Z_0} = \frac{Z_n^{\mathsf{a}}}{Z_0} + \frac{(Z_{n-1}/Z_0)\cos(\beta_{\mathsf{g}}d) + \mathsf{j}\sin(\beta_{\mathsf{g}}d)}{\cos(\beta_{\mathsf{g}}d) + \mathsf{j}(Z_{n-1}/Z_0)\sin(\beta_{\mathsf{g}}d)}.$$
 (2)

We see in (2) that the effective DMA array impedance at the nth element is a combination of the isolated impedance for the nth and the effective DMA array impedance at the previous element transformed by the waveguide transmission line. We can then define the total input impedance for the entire DMA array based on the Nth DMA element impedance in (2) as

$$\frac{Z_{\text{in}}}{Z_0} = \frac{(Z_N/Z_0)\cos(\beta_{\text{g}}d) + j\sin(\beta_{\text{g}}d)}{\cos(\beta_{\text{g}}d) + j(Z_N/Z_0)\sin(\beta_{\text{g}}d)},\tag{3}$$

which fully describes the impedance characteristics of the DMA.

For the reflection coefficient given as $S_{11}=\frac{Z_{\rm in}-Z_0}{Z_{\rm in}+Z_0}$, we define the key performance metrics of return loss as

$$RL = 20\log_{10}|S_{11}| \tag{4}$$

and matching efficiency as

$$e_{\mathsf{m}} = 1 - |S_{11}|^2. \tag{5}$$

Since the input impedance must be calculated recursively from the isolated DMA element impedances, there is not a closed-form solution for the DMA input impedance. Moreover, as (3) is defined by the normalized impedance and the waveguide characteristic impedance is real and positive such that $Z_0 > 0 \in \mathbb{R}$, it is desired for $\frac{Z_{\rm in}}{Z_0} = 1$ to minimize the return loss in (4) and maximize the matching efficiency in (5). We describe an optimization procedure to improve the DMA matching efficiency in Section III-B.

B. DMA beamforming model

Next, we describe the DMA beamforming model and detail the methods to convert a DMA beamforming weight to an isolated impedance. DMAs have a limited antenna weight distribution when compared with phased arrays for beamforming due to the reconfigurable component. The geometry and design of DMA elements are known as complimentary electric LC resonators, which are sub-wavelength in size. The resonant response of the DMA element results in an effective magnetic surface current, which allows for DMA elements to be modeled as point magnetic dipoles [1]. Let F be the coupling factor, and Γ be the damping factor for the magnetic polarizability of a magnetic dipole. The magnetic polarizability expression for a resonant frequency tuning $f_{r,n}$ is given as [1]

$$\alpha_{m,n} = \frac{2\pi f_{t}^{2} F}{2\pi f_{t,n}^{2} - 2\pi f_{t}^{2} + j\Gamma f_{t}}.$$
 (6)

Varying the resonant frequency $f_{r,n}$ around the target frequency f_t changes the magnetic polarizability. For a normalization constant $2\pi f_t \frac{F}{\Gamma}$ on the magnetic polarizability in (6),

the magnetic polarizability at the target frequency is given by a Lorentzian distribution as [1]

$$Q_{\mathsf{dma}} = \left\{ -\frac{\mathsf{j} + e^{\mathsf{j}\varphi}}{2} : \varphi \in [0, 2\pi) \right\}. \tag{7}$$

The distribution in (7) describes the effective DMA antenna beamforming weights as $f_n \in \mathcal{Q}_{dma}$. The reconfigurable resonant frequency $f_{r,n}$ corresponds to a phase φ in (7) to allow for a tunable weight.

We can also extract the magnetic polarizability expression from HFSS simulations based on the isolated scattering parameters S_{11}^{a} , S_{12}^{a} and waveguide design. Let a and b be the waveguide width and height, respectively. The extracted DMA magnetic polarizability is given by [2]

$$\alpha_{m,n} = \frac{\mathrm{j}ab}{\beta_{\mathsf{g}}} \left(1 + S_{11}^{\mathsf{a}}(f_{\mathsf{t}}, f_{\mathsf{r},n}) - S_{12}^{\mathsf{a}}(f_{\mathsf{t}}, f_{\mathsf{r},n}) \right). \tag{8}$$

We can relate a desired DMA weight on the Lorentzian distribution in (7) to the magnetic polarizability in (8) for a designed DMA in HFSS at a resonant frequency tuning. We can then calculate the isolated impedance for this DMA element using (1) with $S_{11}^{\mathsf{a}}(f_{\mathsf{t}}, f_{\mathsf{r},n})$ from simulation results. Further details regarding the mapping from the Lorentzian distribution to a designed DMA are found in [14].

III. IMPEDANCE MATCHING OPTIMIZATION

Given the impedance and beamforming models defined in Section II-A and II-B, we present a technique to improve the impedance match between the DMA and waveguide characteristic impedance. To simplify the implementation and eliminate the need for external hardware or matching networks, we describe a method to increase the matching efficiency solely by configuring the DMA weights.

A. Problem formulation

Our goal is to maximize the DMA matching efficiency in (5) and steer a beam pattern in a desired direction θ_0 using the DMA weights. A phased array with unit-amplitude weights w_n can be configured to steer a beam pattern by setting the weights as $w_n(\theta_0) = e^{\mathrm{j}\frac{2\pi f_t}{c}d\sin\theta_0(n-1)}$, where c is the speed of light. For a DMA, we must account for the addition of the waveguide phase advance β_{g} and configure the weights as $w_n^{\mathrm{dma}}(\theta_0) = e^{\mathrm{j}\frac{2\pi f_t}{c}d\sin\theta_0(n-1)+\mathrm{j}\beta_{\mathrm{g}}d(n-1)}$. Since the DMA weights f_n must lie on the Lorentzian distribution, a simple way to configure DMA weights for beamsteering is to map the unit-amplitude weights w_n^{dma} onto the Lorentzian-constrained weights as [1]

$$f_n(\theta_0) = -\frac{j + e^{j \angle w_n^{\mathsf{dma}}(\theta_0)}}{2}.$$
 (9)

The expression in (9) is known as Lorentzian mapping and was proposed in [1] for beamsteering with DMAs.

We now describe the matching efficiency problem formulation by reconfiguring the set of Lorentzian weights in (9). In any beamforming weight vector with elements $w_n^{\mathsf{dma}}(\theta_0)$, multiplying by a common phase shift $e^{\mathsf{j}\zeta}$ will not change the

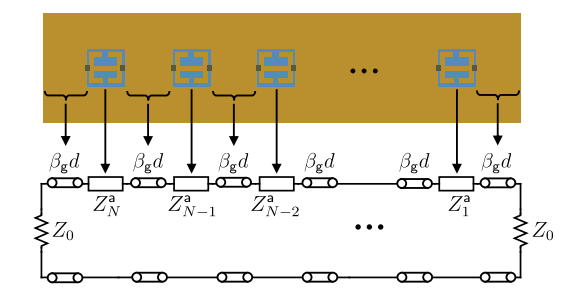


Fig. 1. The equivalent circuit model for an entire DMA array. Each DMA element is modeled as a single, reconfigurable series impedance, while the segments of waveguide in between each element is modeled as a transmission line. The DMA array should be well-matched to the characteristic impedance of the waveguide as Z_0 .

resulting beam pattern. The common phase shift, however, would provide a new set of DMA weights that can change the beam pattern or impedance match when mapped onto the Lorentzian-constrained distribution. This is discussed in further detail in [14]. Since the impedance match changes depending on the configuration of DMA weights, we optimize the DMA weights by determining the common phase rotation ζ applied to the phased-array weights that maximizes the matching efficiency of the mapped DMA weights. We then formulate the DMA matching efficiency optimization problem to maximize matching efficiency while steering a beam pattern in a desired direction θ_0 as

$$\max_{\zeta \in [0,2\pi)} (e_{\mathsf{m}}(\zeta)) \quad \text{s.t.} \quad f_n(\theta_0,\zeta) = -\frac{\mathsf{j} + e^{\mathsf{j} \angle w_n^{\mathsf{dma}}(\theta_0)} e^{\mathsf{j}\zeta}}{2}. \quad (10)$$

We describe the procedure for calculating the optimal phase weight rotation to maximize the matching efficiency in (10) as follows.

B. Impedance matching optimization procedure

We calculate the optimal phase rotation by determining the total impedance using (2) for the set of DMA weights in (10). We outline the steps to calculate the optimal phase rotation as follows:

 Calculate the set of DMA weights from the phased-array solution with the phase rotation as

$$f_n(\theta_0, \zeta) = -\frac{j + e^{j \angle w_n^{\mathsf{dma}}(\theta_0)} e^{j\zeta}}{2}.$$
 (11)

and determine the isolated impedances $Z_n^a(\zeta)$ that correspond to the weights $f_n(\theta_0, \zeta)$ using (8) and (1).

2) Use the recursive impedance algorithm

$$\frac{Z_n(\zeta)}{Z_0} = \frac{Z_n^{\mathsf{a}}(\zeta)}{Z_0} + \frac{(Z_{n-1}(\zeta)/Z_0)\cos(\beta_{\mathsf{g}}d) + \mathsf{j}\sin(\beta_{\mathsf{g}}d)}{\cos(\beta_{\mathsf{g}}d) + \mathsf{j}(Z_{n-1}(\zeta)/Z_0)\sin(\beta_{\mathsf{g}}d)}$$
(12)

to calculate the total input impedance for the DMA array with the set of weights.

3) Determine the reflection coefficient as

$$S_{11}(\zeta) = \frac{Z_{\text{in}}(\zeta) - Z_0}{Z_{\text{in}}(\zeta) + Z_0} \tag{13}$$

from the calculated input impedance.

4) Repeat steps 1-3 for all phase rotations $\zeta \in [0, 2\pi)$ to find the optimal phase rotation ζ^{opt} that maximizes the matching efficiency as

$$\zeta^{\text{opt}} = \underset{\zeta \in [0, 2\pi]}{\operatorname{argmax}} \left(1 - |S_{11}(\zeta)|^2 \right).$$
(14)

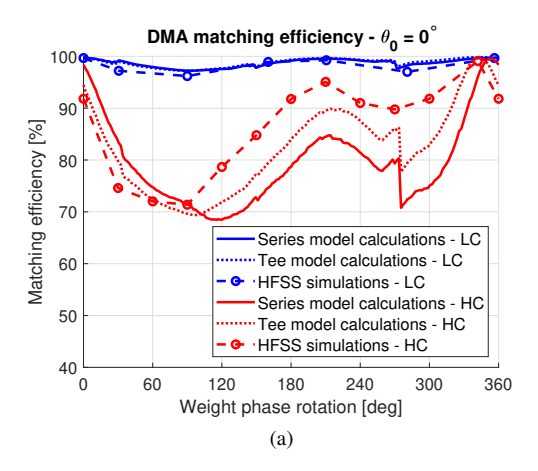
The solution in (14) provides a method to improve the DMA matching efficiency solely by configuring the DMA weights and without any external matching network or additional hardware. In the next section, we determine the impact of the optimization procedure on matching efficiency through simulation results.

IV. SIMULATION RESULTS

We now discuss the effectiveness of the matching optimization procedure for improving the impedance match between the DMA array and the waveguide characteristic impedance. To verify the validity of the impedance model, we design and simulate a DMA in HFSS based on our prior work in [14]. The DMA is designed to operate at $f_{\rm t}=15$ GHz with a spacing of d=6 mm and has N=12 elements. We assume the DMA lies in the xy plane and the elements are spaced along the x axis. To simplify the analysis, we consider a beamsteering scenario and steer a beam pattern at the elevation angles $\theta_0=0^\circ$ and $\theta_0=-30^\circ$. We calculate the DMA weights over all weight phase rotations ζ from (11) to determine the effectiveness of the proposed optimization procedure.

We also consider two DMA designs based on the coupling factor F to investigate how the DMA design impacts the resulting matching efficiency. The coupling factor determines the amount of scattering that occurs within the waveguide due to the DMA element. Larger amounts of scattering leads to bigger variations in the DMA element impedance, depending on the resonant frequency tuning, according to (1), which may decrease the matching efficiency. We alter our initial design in [14] to vary the coupling factor by changing the waveguide height from 1 mm to 4.9 mm, since bigger waveguide heights correspond to lower scattering [4].

We show in Fig. 2 the calculated and simulated matching efficiency for the low coupling (LC) and high coupling (HC) DMA designs at steering angles $\theta_0 = 0^{\circ}$ and $\theta_0 = -30^{\circ}$. We consider calculated results based on both the series and Tee network models. We find in Fig. 2 that for a low coupling DMA design, the DMA is well-matched to the characteristic impedance of the waveguide for both steering angles. This is due to the low amounts of scattering from each DMA element at any resonant frequency tuning, leading to low return loss and matching efficiency greater than 96% over all weight phase rotations. For the DMA design with high coupling, however, the matching efficiency varies greatly across the different weight phase rotations, from around 71% to 99% at $\theta_0 = 0^{\circ}$, and 77% to 94% at $\theta_0 = -30^{\circ}$. This means that the proposed impedance matching optimization procedure can provide a significant increase in the matching efficiency for high coupling DMAs, whereas DMA designs with lower



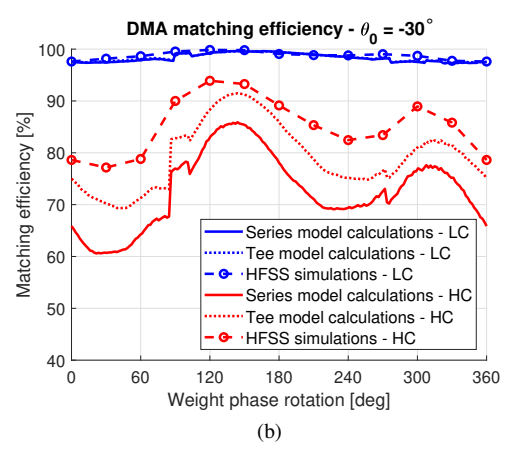
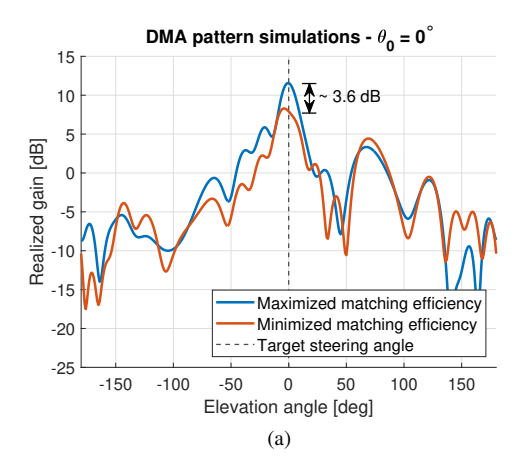


Fig. 2. Calculated and simulated matching efficiency results for a beam steered at (a) $\theta_0 = 0^\circ$ and (b) $\theta_0 = -30^\circ$. We find that for a DMA design with low coupling, the DMA is already very well-matched and the matching efficiency is high. For the DMA design with high coupling, however, the matching optimization procedure provides a significant increase to the matching efficiency across the possible weight phase rotations.

coupling may not require additional matching. Moreover, the differences in the matching efficiency range between the $\theta_0 = 0^{\circ}$ and $\theta_0 = -30^{\circ}$ cases shows how the matching efficiency optimization procedure depends on the desired steering angle.

We also note the agreement between the simulated and calculated results in Fig. 2 to further verify the validity of the impedance models in (1) and (2). While the series and Tee network models for the low coupling design are nearly identical to simulation results, the higher coupling DMA design, however, yields a larger discrepancy between the simulated and calculated results. This is primarily due to mutual coupling and perturbations in the waveguide electromagnetic fields, which is stronger for elements with higher scattering. As expected, for the higher coupling DMA design, the Tee network model provides a slightly more accurate matching efficiency calculation when compared with the series model.

While a DMA design with low coupling may be ideal, larger coupling factors in a DMA design could be necessary due to fabrication limitations. The most simple and low-cost method to fabricate a DMA prototype is through a PCB design using a substrate-integrated waveguide, which means the available



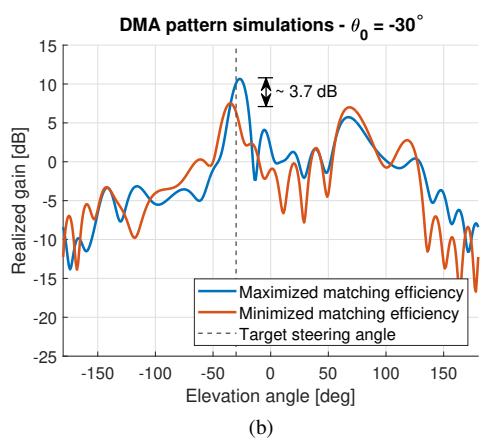


Fig. 3. DMA pattern simulation results for a beam steered at (a) $\theta_0=0^\circ$ and (b) $\theta_0=-30^\circ$ using the DMA design with high coupling. There is a gain difference of approximately 3.6 dB and 3.7 dB between the beam patterns for the weight phase rotations that minimized and maximized matching efficiency.

substrates and layer heights are dictated by the PCB manufacturer. Therefore, if a high coupling factor is unavoidable in a DMA design, the proposed impedance matching optimization method can be used to ensure a good match between the DMA array and the waveguide characteristic impedance.

Next, we show in Fig. 3 the simulated pattern results of the high coupling DMA at both steering angles for the set of weights that maximized and minimized matching efficiency in Fig. 2. We see in Fig. 3 that there is approximately a 3.6 dB and 3.7 dB improvement in the realized gain at the desired steering angles of $\theta_0=0^\circ$ and $\theta_0=-30^\circ$ between the two sets of weights. We also find that the matching efficiency optimization procedure can provide additional performance enhancements in the realized gain that exceed the initial matching efficiency increase. In the $\theta_0 = 0^{\circ}$ case, for example, the matching efficiency difference of 71% to 99% should lead to a realized gain improvement of around 1.4 dB where we instead see a 3.6 dB difference. Moreover, it is important to note that the impedance matching optimization procedure does not require any additional hardware, and can improve both the matching efficiency and realized gain simply by configuring the DMA weights.

V. CONCLUSION AND FUTURE WORK

In this paper, we developed a method to increase the matching efficiency of a DMA array by reconfiguring the DMA element weights based on a common weight phase rotation. We found that for a DMA design with high coupling, the matching efficiency optimization procedure allowed for a large increase in matching efficiency for a beam steered in two directions. The matching efficiency optimization also does not require any external hardware or matching network. In future work, we aim to test our optimization procedure on a fabricated DMA prototype, and consider more sophisticated beamforming and impedance matching optimizations to extend the analysis beyond the Lorentzian-constrained mapping procedure.

VI. ACKNOWLEDGEMENTS

This material is based upon work supported by the National Science Foundation under grant nos. NSF-ECCS-2435261, NSF-CCF-2435254, the Army Research Office under Grant W911NF2410107, and the Qualcomm Innovation Fellowship.

REFERENCES

- [1] D. R. Smith, O. Yurduseven, L. P. Mancera, P. Balanis, and N. B. Kundtz, "Analysis of a waveguide-fed metasurface antenna," *Physical Review Applied*, vol. 8, no. 5, p. 054048, Nov. 2017.
- [2] M. Boyarsky, T. Sleasman, M. F. Imani, J. N. Gollub, and D. R. Smith, "Electronically steered metasurface antenna," *Scientific Reports*, vol. 11, no. 1, pp. 1–10, Feb. 2021.
- [3] N. Shlezinger, O. Dicker, Y. C. Eldar, I. Yoo, M. F. Imani, and D. R. Smith, "Dynamic metasurface antennas for uplink massive MIMO systems," *IEEE Trans. Commun.*, vol. 67, no. 10, pp. 6829–6843, July 2019.
- [4] L. Josefsson and S. R. Rengarajan, Slotted waveguide array antennas: theory, analysis and design. SciTech Publishing, 2018.
- [5] L. Josefsson, "Analysis of longitudinal slots in rectangular waveguides," IEEE Trans. Antennas Propag., vol. 35, no. 12, pp. 1351–1357, Dec. 1987
- [6] G. Stern and R. Elliott, "Resonant length of longitudinal slots and validity of circuit representation: Theory and experiment," *IEEE Trans. Antennas Propag.*, vol. 33, no. 11, pp. 1264–1271, Nov. 1985.
- [7] G. A. Casula, G. Mazzarella, G. Montisci, and G. Muntoni, "A review on improved design techniques for high performance planar waveguide slot arrays," *Electronics*, vol. 10, no. 11, p. 1311, May 2021.
- [8] P. Lu, X.-S. Yang, J.-L. Li, and B.-Z. Wang, "Polarization reconfigurable broadband rectenna with tunable matching network for microwave power transmission," *IEEE Trans. Antennas Propag.*, vol. 64, no. 3, pp. 1136– 1141, Jan. 2016.
- [9] Y. Cai and Y. Jay Guo, "A reconfigurable decoupling and matching network for a frequency agile compact array," in *Proc. 5th Eur. Conf. Antennas Propag. (EUCAP)*, Apr. 2011, pp. 896–899.
- [10] H.-Y. Li, C.-T. Yeh, J.-J. Huang, C.-W. Chang, C.-T. Yu, and J.-S. Fu, "Cpw-fed frequency-reconfigurable slot-loop antenna with a tunable matching network based on ferroelectric varactors," *IEEE Antennas Wireless Propag. Lett.*, vol. 14, pp. 614–617, Dec. 2014.
- [11] E. Arabi, K. A. Morris, and M. A. Beach, "Analytical formulas for the coverage of tunable matching networks for reconfigurable applications," *IEEE Trans. Microw. Theory Techn.*, vol. 65, no. 9, pp. 3211–3220, Apr. 2017.
- [12] D. R. Smith, M. Sazegar, and I. Yoo, "Equivalence of polarizability and circuit models for waveguide-fed metamaterial elements," arXiv preprint arXiv:2406.06102, Jun. 2024.
- [13] D. M. Pozar, Microwave engineering: theory and techniques. John wiley & sons, 2021.
- [14] J. Carlson, M. R. Castellanos, and R. W. Heath, "Hierarchical codebook design with dynamic metasurface antennas for energy-efficient arrays," *IEEE Trans. Wireless Commun.*, vol. 23, no. 10, pp. 14790–14804, Jul. 2024.